Reducing the melting and sublimation of the galvanized sheets zinc layer during the laser beam cutting

IOP Conf. Series: Materials Science and Engineering **393** (2018) 012096 doi:10.1088/1757-899X/393/1/012096

Reducing the melting and sublimation of the galvanized sheets zinc layer during the laser beam cutting

J Meško[1], R Nigrovič[1] and R Nikolić[2,3]

[1]University of Žilina, Faculty of Mechanical Engineering, Univerzitná 1, 010 26 Žilina, Slovakia
[2]University of Žilina, Research Center, Univerzitná 1, 010 26 Žilina, Slovakia
[3]University of Kragujevac, Faculty of Engineering, Sestre Janjić 6, 34000 Kragujevac, Serbia

E-mail: rastislav.nigrovic@fstroj.uniza.sk

Abstract. The presented research is dealing with principles and technology of the laser cutting. The properties of the CO_2 laser beam, input parameters of the laser cutting, assist gasses, interaction with the cut material and the cutting process stability are described. Influence of the heat from the laser beam on degradation of the zinc surface layer, which serves as the anti-corrosive protection of the lower carbon steel, is considered in this paper. In the experimental part of this research, the two most important laser cutting parameters were experimentally changed, namely the type of the assist gas - O_2 and N_2 and the cutting speed.

1. Introduction

The principle of the laser cutting of metallic materials is based on the action of a focused laser beam on the cut material. In material cutting in the technical practice, the surface, to which is the laser beam incoming, is in the form of a circle with diameter of 0.1 to 0.4 mm, depending on the structure of the device and the thickness of the cut material. The laser beam of the above-mentioned parameters impacting on the cut material causes its rapid heating, Figure 1. The cut material is in within milliseconds heated to the melting point or to the evaporation temperature. When the laser beam impacts the cut material, a mutual interaction occurs between the cut material and the beam itself. The subsequent phenomena, occurring during the material cutting, which are affecting the properties of the material after the impact of the focused beam, depend, in particular, on the chemical composition of the cut material and on the quality of its surface [1, 6, 7].

2. Interaction of the laser beam and the cut material

In the thermal separation of metallic materials by the laser, it is always necessary first to create a hole in the workpiece, from which the cutting is continued. The formation of the opening is based on the laser-drilling principle and has a slightly different course characteristics than the cutting itself. The incident laser beam transmits the kinetic energy of the photons of the material, which converts to heat that melts and partially vaporizes the heated material, Figure 2 [1, 2, 5].

In the melt laser cutting process, the material is heated locally above the melting point, with a stream of pure inert gas, which removes the material from the cutting point, but does not affect the cutting process itself. Material separation takes place in the liquid phase, so the process in question is the melt cutting by a laser. The cutting gas is usually nitrogen, though the noble gases could also be used,

Figure 1. Photo of the laser cutting process.

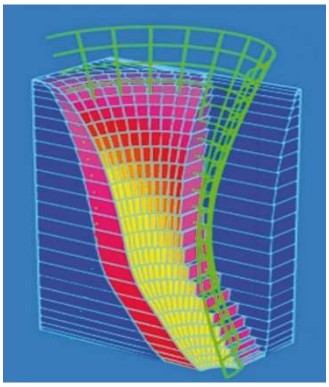

Figure 2. The laser cutting simulation.

depending on the cutting workpiece or the cut quality requirements. The lower cutting head feed rates may also be used, as with other laser cutting methods. The maximum cutting speed increases linearly with the laser power and decreases approximately linearly with the thickness of the cut material and the corresponding melting temperature of the material. In that case, the laser beam is poorly absorbed. The quality of the cut is impaired by the molten slag on the lower edge of the cut. That slag must be removed. The higher surface roughness is also achieved. Said method is suitable, in particular for forming the non-oxidized cuts of metallic materials, for instance anti-corrosive steels, Al, brass and galvanized sheet metal [3, 4].

In an oxidative laser cutting process, the material at the point of the laser beam impact is heated to the ignition temperature and burnt in the flow of the active oxygen gas. The oxidative effect is manifested by the initial oxidation of the laser beam (by decreasing the light reflection coefficient), as well as by the additional exothermic reaction heat of combustion, which ensures an increase in the cutting speed. The cutting process is therefore the result of an exothermic reaction of the material with oxygen [3, 8].

3. Experimental material

The test specimens were made on the Lasercell 1005 laser cutting machine (Trumpf) for material - Steel 1.0355 + Z (thickened steel with zinc coating) of thickness t = 2 mm, Tables 1 and 2.

Table 1. Mechanical properties of the 1.0355 steel.

R_e [MPa]	R_m [MPa]	A_{80} [%]
140 – 260	270 – 380	≥ 30

Table 2. Chemical composition of the 1.0355 steel.

Maximum values in %					
C	Si	Mn	P	S	Ti
0.12	0.5	0.6	0.1	0.045	0.3

4. Experimental conditions and experiments evaluation

Experimental samples of 1.0355 steel were cut with application of the two distinct gases - inert N_2, and active, strongly oxidizing O_2. For each of the used gasses the constant laser cutting parameters were appropriately set. The varying parameter was the cutting speed, which was within range 6.6 m/min – 2.4 m/min for N_2 and 4.95 m/min – 1.8 m/min for O_2. The evaluation criterion for amount of the heat-deteriorated zinc coating was the width of the molten and extruded zinc layer, done by measurement and the immersion corrosion test.

Sample No. 1 (Figures 3 and 4)
Cutting parameters

- Cutting speed – 6.6 m/min,
- Assist gas – N_2,
- Nozzle diameter – Ø 1.4 mm,
- Power – 4000 W,
- Gas pressure – 1.6 MPa,
- Focusing point position – 1 mm.

The measured mean value of the width of the heat-sublimed and molten zinc area on the input surface of the laser beam penetration ΔL_1 and on the laser beam output surface ΔL_2 were:

$$\Delta L_1 = 0.773 \text{ mm and } \Delta L_2 = 0.41 \text{ mm.}$$

After the corrosion test, carried out in 3% NaCl solution for 35 days, the corrosion mass decreased the original weight by 1.86690%.

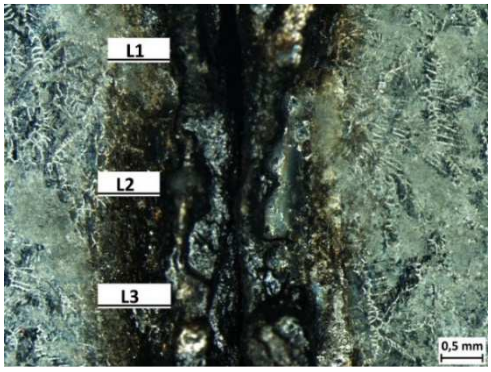

Figure 3. Laser beam penetration area of sample # 1.

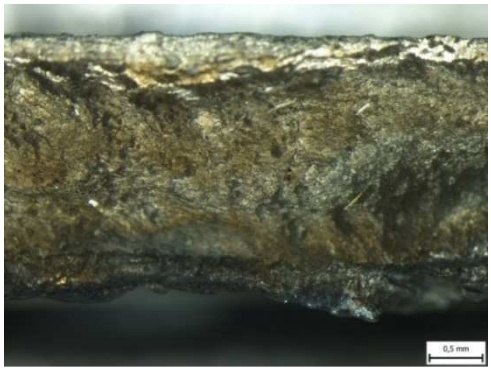

Figure 4. The cut edge surface of sample # 1 after the corrosion test.

Sample No. 2 (Figures 5 and 6)
Cutting parameters

- Cutting speed – 4.8 m/min,
- Assist gas – N_2,
- Nozzle diameter – Ø 1.4 mm,
- Power – 4000 W,
- Gas pressure – 1.6 MPa,
- Focusing point position – 1 mm.

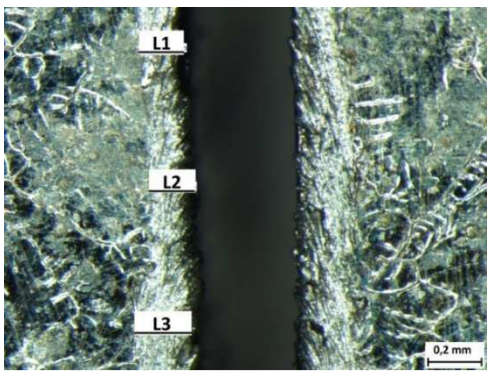

Figure 5. Laser beam penetration area of sample # 2.

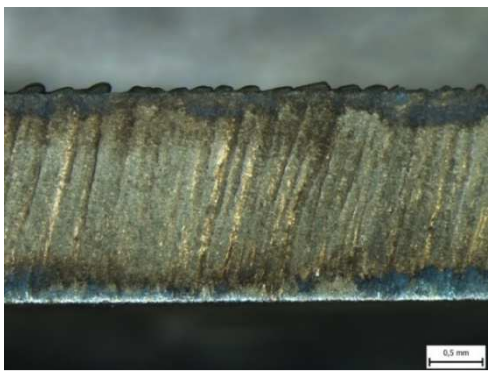

Figure 6. The cut edge surface of sample # 2 after the corrosion test.

The measured mean value of the width of the heat-sublimed and molten zinc area on the input surface of the laser beam penetration ΔL_1 and on the laser beam output surface ΔL_2 were:

$$\Delta L_1 = 0.163 \text{ mm and } \Delta L_2 = 0.41 \text{ mm.}$$

After a corrosion test, carried out in 3% NaCl solution for 35 days, the corrosion mass decreased the original weight by 1.68853%.

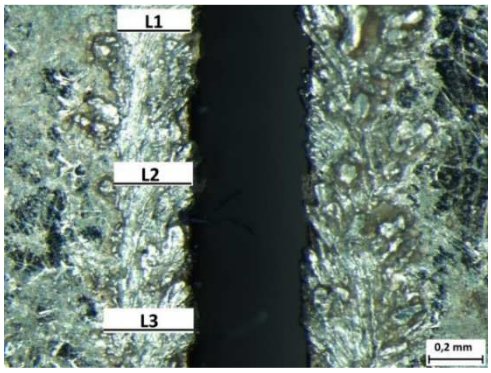

Figure 7. Laser beam penetration area of sample # 3.

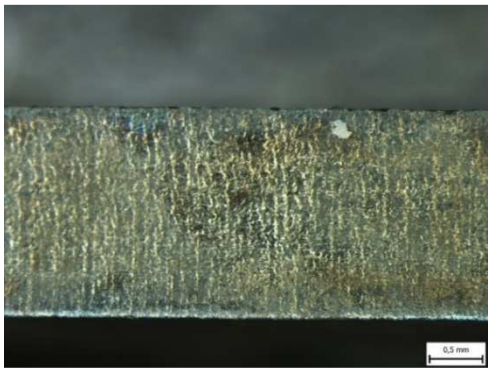

Figure 8. The cut edge surface of sample # 3 after the corrosion test.

Sample No. 3 (Figures 7 and 8)
Cutting parameters

- Cutting speed – 2.4 m/min,
- Assist gas – N_2,
- Nozzle diameter – Ø 1.4 mm,
- Power – 4000 W,
- Gas pressure – 1.6 MPa,
- Focusing point position – 1 mm.

The measured mean value of the width of the heat-sublimed and molten zinc area on the input surface of the laser beam penetration ΔL_1 and on the laser beam output surface ΔL_2 were:

$$\Delta L_1 = 0.29 \text{ mm and } \Delta L_2 = 0.437 \text{ mm.}$$

After the corrosion test, carried out in 3% NaCl solution for 35 days, the corrosion mass decreased the original weight by 1.53703 %.

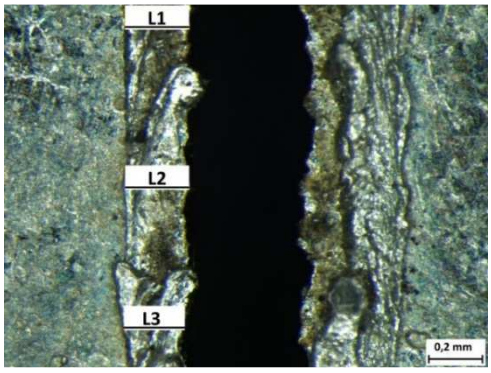

Figure 9. Laser beam penetration area of sample # 4.

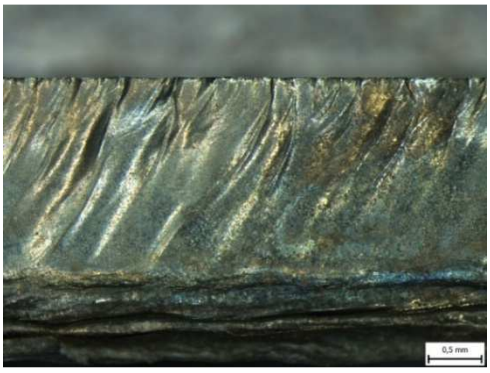

Figure 10. The cut edge surface of sample # 4 after the corrosion test.

Sample No. 4 (Figures 9 and 10)
Cutting parameters

- Cutting speed – 4.95 m/min,
- Assist gas – O_2,
- Nozzle diameter – Ø 1.0 mm,
- Power – 1200 W,
- Gas pressure – 0.35 MPa,
- Focusing point position – 1 mm.

The measured mean value of the width of the heat-sublimed and molten zinc area on the input surface of the laser beam penetration ΔL_1 and on the laser beam output surface ΔL_2 were:

$$\Delta L_1 = 0.227 \text{ mm and } \Delta L_2 = 0.45 \text{ mm.}$$

After the corrosion test, carried out in 3% NaCl solution for 35 days, the corrosion mass decreased the original weight by 1.31170%.

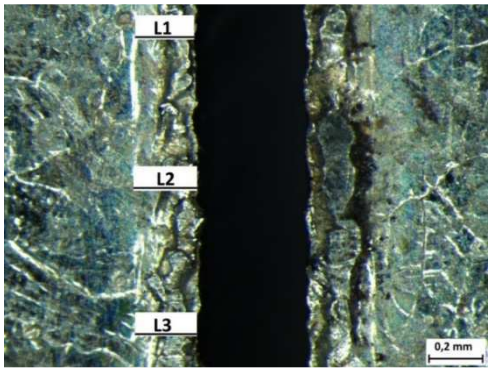

Figure 11. Laser beam penetration area of sample # 5.

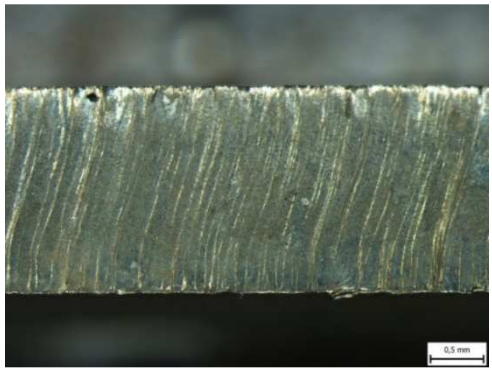

Figure 12. The cut edge surface of sample # 5 after the corrosion test

Sample No. 5 (Figures 11 and 12)
Cutting parameters

- Cutting speed – 6.6 m/min,
- Assist gas – O_2,
- Nozzle diameter – Ø 1.0 mm
- Power – 1200 W,
- Gas pressure – 0.35 MPa,
- Focusing point position – 1 mm.

The measured mean value of the width of the heat-sublimed and molten zinc area on the input surface of the laser beam penetration ΔL_1 and on the laser beam output surface ΔL_2 were:

$$\Delta L_1 = 0.227 \text{ mm and } \Delta L_2 = 0.26 \text{ mm.}$$

After the corrosion test carried out in 3% NaCl solution for 35 days, the corrosion mass decreased the original weight by 2.03539 %.

Sample No. 6 (Figures 13 and 14)
Cutting parameters

- Cutting speed – 1.86 m/min,
- Assist gas – O_2,
- Nozzle diameter – Ø 1.0 mm
- Power – 1200 W,
- Gas pressure – 0.35 MPa,
- Focusing point position – 1 mm.

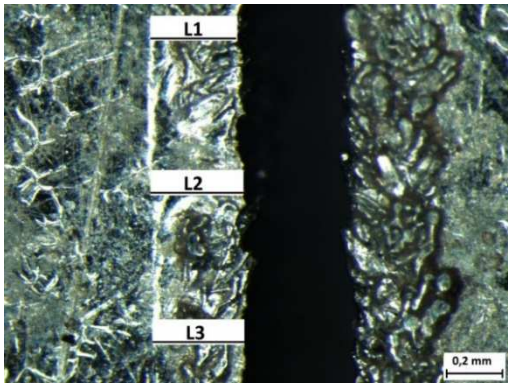

Figure 13. Laser beam penetration area of sample # 6.

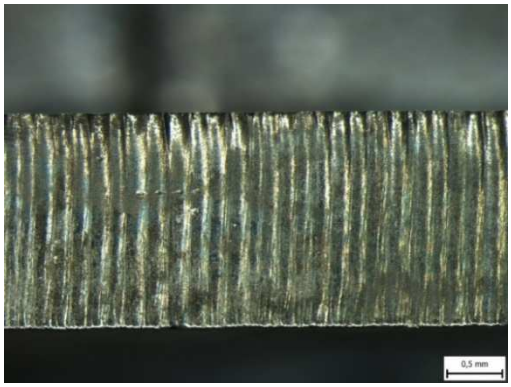

Figure 14. The cut edge surface of sample # 6 after the corrosion test.

The measured mean value of the width of the heat-sublimed and molten zinc area on the input surface of the laser beam penetration ΔL_1 and on the laser beam output surface ΔL_2 were:

$$\Delta L_1 = 0.313 \text{ mm and } \Delta L_2 = 0.203 \text{ mm.}$$

After the corrosion test carried out in 3% NaCl solution for 35 days, the corrosion mass decreased the original weight by 1.63677 %.

Summary diagrams of the cutting speed on area of the heat degraded zinc layer for application of N_2 and O_2 are presented in Figures 15 and 16, respectively.

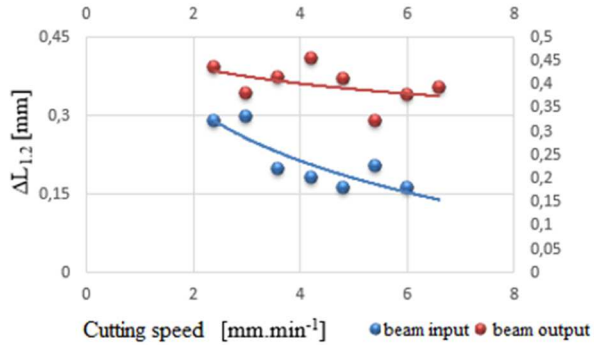

Figure 15. Influence of the cutting speed on area of the heat-degraded zinc layer with N_2 application.

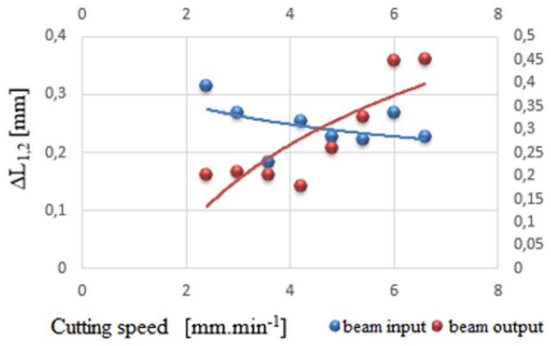

Figure 16. Influence of the cutting speed on area of the heat-degraded zinc layer with O_2 application.

From the graphical evaluation of the experimental measurement, it can be concluded that the width of the area of the heat-deteriorated zinc layer on the surface of samples decreases with the increasing N_2-gas cutting rate. This fact can be explained by the amount of heat introduced at different speeds.

With application of the O_2 gas, the output values of the heat-degraded zone of the zinc layer vary, with respect to application of N_2. On the surface of the laser beam input, degradation with an increasing cutting speed is increasing. The outlet width of the de-zinc layer decreases again. This fact can be explained by influence of the exothermic reaction, as the material did not melt but burned, which caused a wider influence on the lower part of the cut.

Mass losses after the dip corrosion test (3 % NaCl, 35 days) for the two gasses applications are presented in Figure 17.

The resulting graphical evaluation of the immersion corrosion test, by weight loss of samples, has shown that decreasing the rate of laser cutting together with the use of the N_2 gas, aids slightly in degradation of the zinc layer, thereby promoting the anticorrosive properties of the cut material. Laser

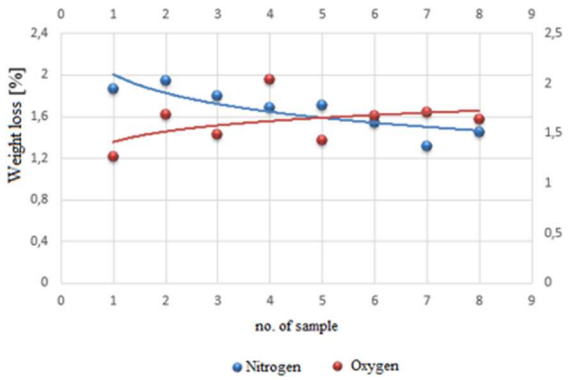

Figure 17. Mass losses after a dip corrosion test (3% NaCl, 35 days).

cutting using the O_2 gas, with decreasing cutting speed, on the contrary, aggravates the anticorrosive properties of the material. The surface of the cut, however, contains oxides, which serve as anticorrosive protection, which during the corrosion test, impeded the corrosion process, but was removed from the point of the cut when the corrosive waste was cleaned.

5. Simulation of the laser cutting process

An introductory step for creating a model of the laser cutting process is a compact analysis of the problem and the definition of the result, especially from that point of view, so that it is clear what is required from the simulation. An important step is to correctly define the total heat source, respectively, the heat, which is then dispersed in the surrounding material. Said method of defining a heat source is performed based on the mathematical relationship in which the coefficient of reflectivity of the surface to which the laser beam enters, the coefficient of energy absorption of the photon flux through the material and the analytical function representing the 2D Gaussian curve are included as variables. That equation defines a point thermal source. The next step is to determine the correct networking of the model. The point heat source, which represents the power of the photons moving in the laser beam, is defined as the boundary condition in the entire domain in the simulated design.

The simulation was generated as a process of heating the plate. The material properties of the board are considered to be constant - simulation does not involve a change in the material phase. The refractive index of the steel is defined by the reflection coefficient and the energy absorption coefficient of the material. The material model represents a plate whose sides except the top are considered to be heat insulated. The movement of the laser beam is characterized by the x and y coordinates, and in the xy plane, $z = 0$ is on the surface of the plate. Parameters x_0 and y_0 serve to enter the shift of the center of the laser beam. The diameter of the incident laser beam in practice has a changing value, the shifting of the laser beam focus point, and therefore the change of the incident beam diameter is defined by the standard deviation parameters σ_x and σ_y.

Variables used for simulation:

- Material: 1.0355 + Z,
- Assist gas: O_2 3.5,
- Power: 3.2 J/mm,
- Cutting speed: 4.5 m/min,
- The dimension of the plate: 80 mm,
- Thickness of the plate: 2 mm,
- The dimension of the mesh square: 0.15 mm,
- The dimension of the kerf: 0.25 mm,
- Calculation step: 0.1 s,
- The end of simulation: 10 s,
- The time of the laser beam on the plate: 0.8 s,
- Cooling: air 20 ºC.

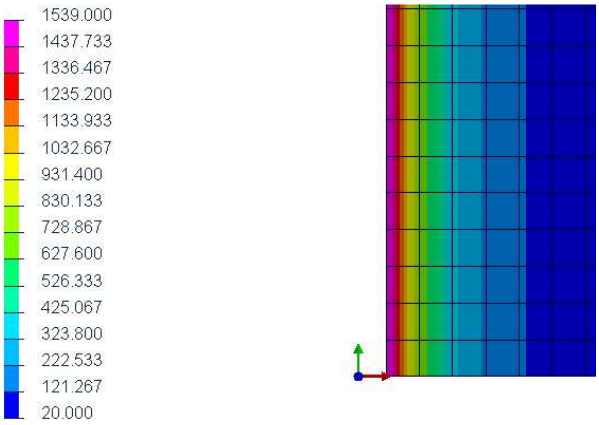

Figure 18. Simulation of thermal influence.

Based on the model of the heat transfer in the material during the laser cutting, it is possible to understand the principle of the heat conduction from the cutting point to the surrounding material. This mechanism is especially important when dealing with the problem of cutting the rough metal sheets, with a complicated cutting path so that a relatively large amount of heat is introduced into the material. Based on the analysis of the simulated model results, it can be stated that the temperature of the material, at the point of cutting at the edge of the laser beam, is assumed to be approximately 1540 °C, Figure 18. The maximum stress, due to the thermal expansion of the material is assumed to be approximately 650 MPa, Figure 19. The temperature of the material at the cutting location is relatively high, but with increasing the distance from the cutting point it drops sharply.

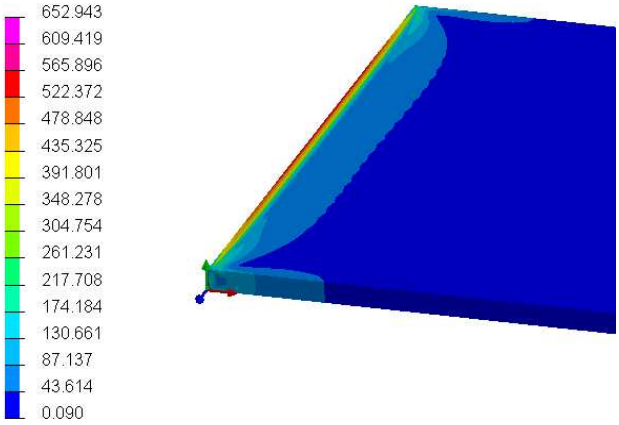

Figure 19. Simulation of Von Mises residual stresses.

6. Conclusion

The present paper analyzes and compares the influence of the cutting speed and the type of the assist laser gas on the corrosion properties and degradation of the zinc layer of the galvanized sheets.

Based on the analysis of the results of the experimental measurements, it can be stated that the degradation of the zinc layer of the galvanized sheets, and thus the corrosion at the cutting location, can be eliminated by suitably setting parameters of the laser cutting. Simulation of the laser cutting of the galvanized material revealed the heat fields in the laser cutting and showed the method of cooling the cut material and the method of melting, sublimation and degradation of the zinc coating. Subsequently it displays the residual Von Misses stress.

Acknowledgement
This research was financially supported by European regional development fund and Slovak state budget by the project "Research Centre of the University of Žilina" and by the KEGA 014ŽU-4/2016 project, led by the principal investigator prof. Ing. Jozef Meško, PhD.

References

[1] Kovalev O B 2010 Actual Principles of the Simulation of State-of-the-Art Technologies of Laser Processing of Materials, *Proceedings of SPIE* **7996** 799602-1–799602-11
[2] Danielewski H, Banak R and Domagala A 2013 *The Experimental Analysis of Striation Pattern Created During Laser Cutting*, 10th European Conference of Young Researchers and Scientists TRANSCOM, Žilina, Slovakia, June 24-26, pp. 23-26
[3] Mucha Z and Mulczyk K 2013 Modeling and Experimental Investigations of Keyhole Laser Welding, *Proceedings of SPIE* **8703** 87030U-1–87030U-9
[4] Koňár R, Patek M and Mičian M 2014 *Numerical Simulation of Arc Welding in Simulation Programme SYSWELD*, 5th International Technical Conference – Technological Forum, Kouty, Czech Republic, June 17-19, pp. 66-70
[5] Zapoměl J, Dekýš V, Ferfecki P, Sapietová A, Sága M and Žmindák M 2015 Identification of Material Damping of a Carbon Composite Bar and Study of Its Effect on Attenuation of Its Transient Lateral Vibrations, *International Journal of Applied Mechanics* **7**(6) 1550081-1–1550081-18
[6] Rózowicz S, Tofil S and Zrak A 2016 An Analysis of the Microstructure, Acrostructure and Microhardness of Nicr-Ir Joints Produced by Laser Welding with and Without Preheat *Archives od metallurgy and materials* **61**(2b) 1157-1162
[7] Fabian P, Zrak A 2016 Evaluation of Selected Properties of Steel 100Cr6 At Different Ways of Heat Treatment, *Manufacturing Technology: Journal for Science, Research and Production* **16**(4) 687-691
[8] Kurp P, Bank R, Mulczyk K and Zrak A 2017 *FEM Numerical Analysis of Thermal Field Distribution and Experimental Study of Circumferenital Laser Welding of Thin-Walled Aluminium Alloy Pipes*, International Conference on Metallurgy and Materials METAL, Brno, Czech Republic, May 24-26, pp. 894-899